J. Mol. Model. **1996**, *2*, 175 – 182

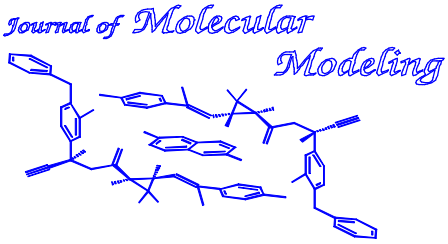

Solvation Effects on the Conformational Behaviour of Gellan and Calcium Ion Binding to Gellan Double Helices

Vivienne L. Larwood, Brendan J. Howlin*, Graham A. Webb

Dept. of Chemistry, University of Surrey, Guildford, Surrey, GU2 5XH, UK (chs1bh@surrey.ac.uk)

Received: 13 March 1996 / Accepted 04 June 1996 / Published: 21 June 1996

Abstract

The contribution of the presence of solvent to the conformations adopted by disaccharide fragments within the repeat unit of gellan have been studied by molecular modelling techniques. Initial conformational energy searches, using a dielectric continuum to represent the solvent, provided starting geometries for a series of molecular dynamics simulations. The solution behaviour from these simulations was subsequently compared to fibre diffraction data of the potassium gellan salt. The present calculations indicate considerable flexibility of the glycosidic linkages, and this is discussed in relation to its effect on gel formation. One of the fragments was solvated with explicit water molecules. These calculations showed the same conformational behaviour as those simulations conducted in implicit solvent.
Finally, a series of molecular dynamics (MD) simulations were performed to study the calcium binding to gellan. The results from this clearly showed a well defined binding site for this ion.

Abbreviations: MM : molecular mechanics; MD : molecular dynamics.
Keywords: polysaccharides, gellan, glycosidic linkage.

Introduction

Gellan is an anionic, microbial polysaccharide with the basic repeat unit of (1→3)-β-D-Glc*p*-(1→4)-β-D-Glc*p*A-(1→4)-β-D-Glc*p*-(1→4)-α-L-Rha*p* [1]. A schematic of the gellan repeat unit can be found in Figure 1. Its ability to form firm aqueous gels at low polysaccharide concentration in the presence of specific counter ions has led to its use as a thickening agent in a variety of food applications. Its affects have been studied in food systems as diverse as dairy products [2] to corn syrups [3] and low sugar bakery jams [4].

Several groups have studied the dilute solution behaviour of gellan, using a variety of counter ions, with a view to gaining some insight into the process of gel formation [5-13]. These have mainly concentrated on measuring gel strengths under different conditions of counter ion type and concentration, temperature, polysaccharide concentration and pH. The aim of this work is to study the effect of solvent on the conformational properties of the gylcosidic linkages within the gellan repeat unit and to use a combined molecular mechanics (MM) and molecular dynamics (MD) approach to investigate the co-ordination of divalent ions to the gellan double helix, using Ca^{2+} ions as an example.

Polysaccharides have received relatively little attention from computational studies compared to other macromolecules, such as proteins. Both groups suffer from similar difficulties, such as the current inability to predict conformation based solely on primary structure. However, progress is being made. So far, in the case of polysaccharides, this has

* *To whom correspondence should be addressed*

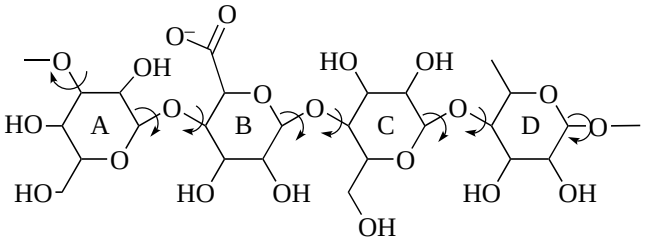

Figure 1. *Schematic representation of gellan with residue labelling.*

mainly concentrated on analysing individual glycosidic linkages. We use this type of approach to validate the model and force field used in subsequent calculations.

We are well aware that modelling the entire time sequence leading to gelation from a disordered aqueous solution is beyond the scope of current simulation methods. It is also impractical at present to simulate models which are of a sufficient size to represent all aspects of gel formation. Therefore we have decided to concentrate on one stage of the pathway, which is where double helices have formed and are in close proximity to each other. In this simulated state the specific interactions with the counter ions can be probed in detail without the need to attempt to model the formation of the gel.

Methodology

General

All calculations were performed on a Silicon Graphics Iris Indigo XZ 4000 workstation. The molecular modelling package INSIGHT II Version 2.3.0 (Biosym Technologies, San Diego, CA, USA) was used to construct all models, and the INSIGHT II interface to Discover Version 2.95 was utilised for the calculations on the structures. The AMBER force field [14] with the modifications for polysaccharides by Homans [15] was used in all simulations.

The explicit image protocol was used in all MD simulations, as was the Verlet algorithm [16]. A step size of 1 femtosecond was used in all of the MD simulations.

All simulations using periodic boundary conditions were conducted under conditions of constant temperature and volume. The temperature is maintained using Berendsen's method [17], which couples the system to a temperature bath.

Conformational Energy Maps

Relaxed conformational energy maps were calculated by restraining the φ and ψ dihedral angles and energy minimising the remaining structure around these dihedral angles. The dihedral angles involved in this study have been shown in Figure 1. For the (1→4) linkages φ is defined as H1-C1-O1-C4', and ψ is defined as C1-O1-C4'-H4', where a prime symbol indicates the following residue. For the (1→3) linkages, φ is defined as H1-C1-O1-C3', and ψ is defined as C1-O1-C3'-H3'. Initially, both of the dihedral angles were set to -180º, and the structures were energy minimised. The dihedral angle ψ was then incremented by 30º, while φ was held constant, and the energy minimisation procedure was repeated. This was then repeated until the dihedral angle ψ had swept out 360º; the dihedral angle φ is then incremented by 30º and the whole procedure was again repeated until each of the dihedral angles had been rotated by the full 360º for all values of the other.

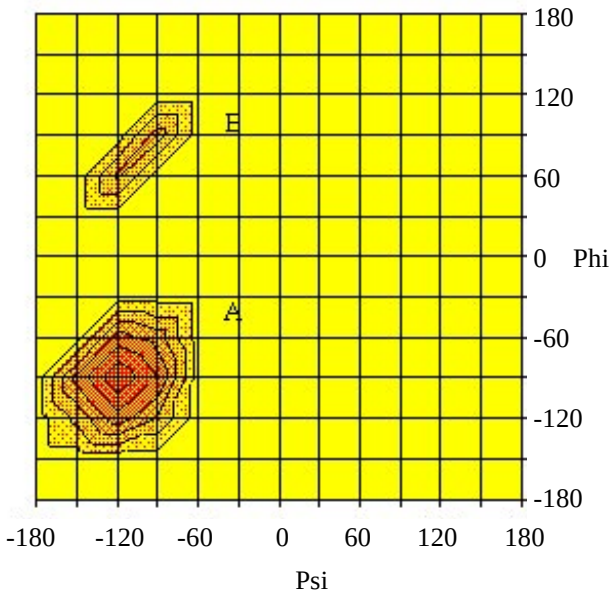

Figure 2. *Conformational energy search for the A-B glycosidic linkage.*

Disaccharide Simulations with Dielectric Constant

The minimum energy conformations predicted by these relaxed conformational energy maps were subsequently used as the starting structures for 500 picoseconds MD simulations. This procedure has been described by Stern et al. [18]. Cut-offs for the non-bonding interactions were not used in these calculations with the disaccharide fragments, as the molecules under consideration were relatively small.

A relative dielectric constant of 80 was used to implicitly represent the presence of solvent. Some representation of solvent effects is essential when modelling polysaccharides, due to their strong tendency to form hydrogen bonds. The MD simulations were run at a temperature of 295K. There was an initial 50 picoseconds equilibration; the subsequent 500 picoseconds of the trajectory were used for the data collection.

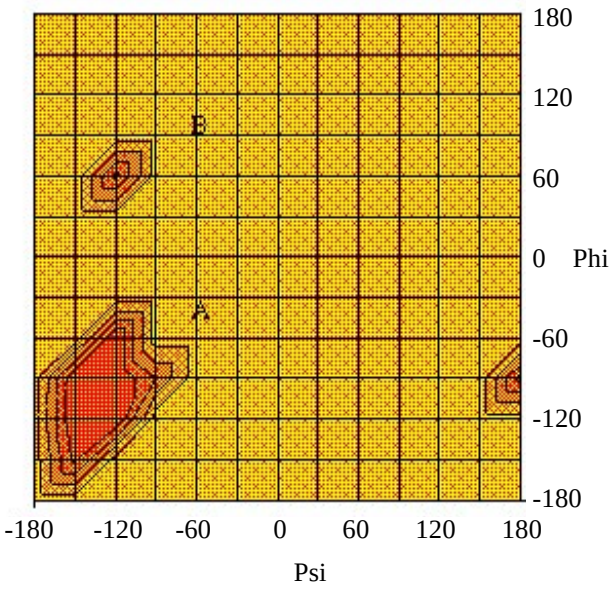

Figure 3. *Conformational energy search for the B-C glycosidic linkage.*

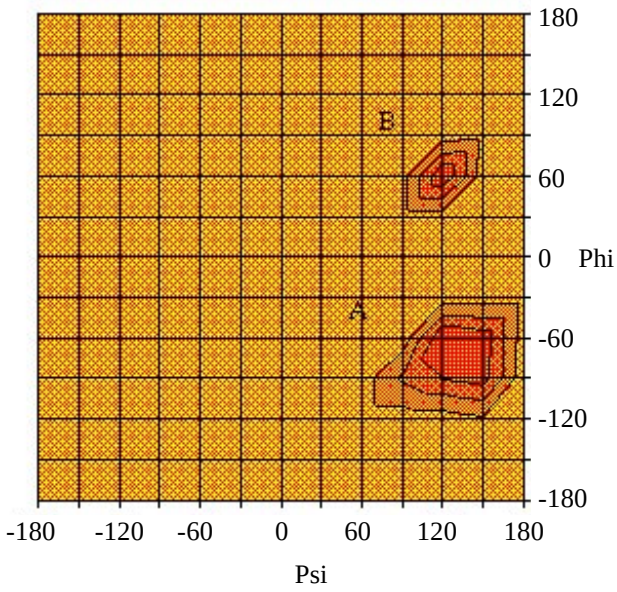

Figure 4. *Conformational energy search for the C-D glycosidic linkage.*

Disaccharide Simulations in Explicit Water

One of the disaccharides also underwent a MD simulation in the presence of explicit water molecules, to determine the effect this may have on the minimised structure from the calculations in vacuum. The disaccharide was solvated using a 15Å^3 box of equilibrated water molecules. The TIP3P model of water [19] was used in all simulations. The TIP3P has recently been successfully used in MD simulations with sucrose [20]. The waters were placed randomly around the disaccharide, whilst avoiding any steric over-laps. This resulted in a total of 84 water molecules.

In this particular system, cut-offs were employed for the non-bonding interactions at 15Å, since periodic boundary conditions were required to contain the water molecules. A group based switching function smoothly adjusted the potential to zero over a 1.5Å range.

Double Helix Simulations Without Ions

Gellan gels consist of rigid, crystalline regions of aggregated double helices [21], linked by more flexible segments [9]. The model system has been developed to represent the interactions present within the crystalline regions only. This reduced size model consists of two double helices. The two strands of each double helix are composed of just four pyranose rings. This represents the repeat unit of the polysaccharide chains, and is the minimum required to model the cation binding. These systems are fully solvated with explicit water molecules to model more accurately the small scale interactions, such as hydrogen bonding, and to include the solvation shell around the ions.

These simulation cells have the dimensions a = 26.0, b = 22.0, c = 35Å with the angles $\alpha = \beta = \gamma = 90^o$. This is slightly larger than the unit cell dimensions of a = b = 15.8, c = 28.2Å, to allow for full solvation of the polysaccharide chains. The waters are placed randomly around the chains, in the same way as described for the disaccharide fragments. This resulted in a total of 185 water molecules.

As before, a step size of 1 femtosecond was chosen. The systems are judged to have equilibrated sufficiently when the total fluctuation of the temperature is less than 5º about the target temperature, and the ratio of potential energy to kinetic energy remains constant. These indicate that the system has reached thermal equilibrium.

Double Helix Simulations With Ions

The Ca^{2+} ions are initially placed arbitrarily in positions close to the carboxyl groups between the polysaccharide chains, and it is from these positions that they move into the coordination sites proposed by Chandrasekaran [21] during subsequent energy minimisation of the systems. The proposed binding site itself involves two carboxyl groups, one from each of the double helices. Thus the ions are believed to bridge between the double helices, rather than within a double helix.

The systems were first minimised, holding the chains rigidly fixed in space, to enable the water molecules to orient themselves with respect to the other atoms in the system. 10 picoseconds intervals of MD were also used to distribute the

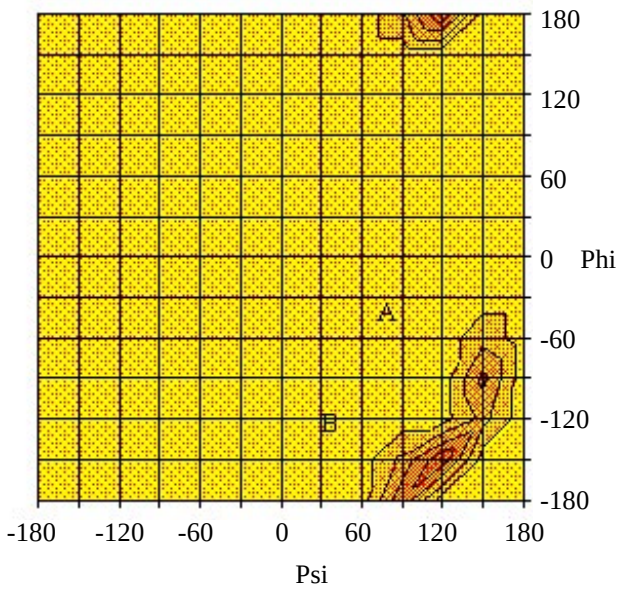

Figure 5. *Conformational energy search for the D-A glycosidic linkage.*

water molecules more evenly around the simulation cell. During this process, the polysaccharides and ions were held in position, and the temperature used was 295K.

The complete systems were then relaxed using steepest descents and conjugate gradient energy minimisation. A total of 200 picoseconds was used for the equilibration process; this included 80 picoseconds each at 100K and 200K and finally 40 picoseconds at 295K. The following 200 picoseconds of the trajectory, at a temperature of 295K, was then collected and analysed. Structures were saved every 500 femtoseconds. The final simulation temperature was 295K. This is the normal temperature of use for gellan products. It should be noted that the actual temperature at which gellan gels deteriorate depends on the concentration of gellan and the nature and concentration of the counter ions present [7].

Table 1. *Comparison between the fibre diffraction data for the glycosidic linkages and the results from both the M.M. and M.D. calculations.*

Dihedral angle	Dihedral angle (º) fibre diffraction data	Dihedral angle (º) conformational energy searches	Dihedral angle (º) molecular dynamics simulations.
O5D-C1D-O3A-C3A	-124	-150	$-180 < \theta < -150$: $150 < \theta < 180$
C1D-O3A-C3A-C4A	88	120	$90 < \theta < 120$
O5A-C1A-O4B-C4B	-101	-90	$-100 < \theta < -70$
C1A-O4B-C4B-C5B	-136	-120	$-150 < \theta < -90$
O5B-C1B-O4C-C4C	-154	-90	$-120 < \theta < -30$
C1B-O4C-C4C-C5C	-144	-120	$-180 < \theta < -90$
O5C-C1C-O4D-C4D	-150	-90	$-120 < \theta < -60$
C1C-O4D-C4D-C5D	86	120	$60 < \theta < 120$

Results

Structural data for polysaccharide gels can often be particularly difficult to obtain; a general lack of crystallinity precludes the use of X-ray crystallography, whilst solution NMR often yields only rotationally averaged conformations. In favourable cases, such as gellan, it may be possible to extract fibres in which the molecules are preferentially oriented in the same direction [22]. From such samples it is then possible to obtain fibre diffraction data; although this is not as precise as X-ray crystallography, it can nevertheless provide sufficient details of the structure to determine unit cell dimensions, helix pitch and possibly even the location of specific crystalline water molecules. Such data provide useful starting structures for atomistic simulations. In the case of gellan, this type of data was obtained by Chandrasekaran et al. for both the lithium [23] and the potassium [21] salt of gellan. The fibre diffraction data for the potassium salt were used for the starting structure of the double helices. These data are also used for comparison with calculated results for the disaccharide fragments. These calculations were performed as described in the methodology section.

Conformational Energy Maps

The results from the conformational energy searches and subsequent MD calculations performed here on all four of the glycosidic linkages have been compared to the fibre diffraction values, and listed in Table 1. As can be seen, there is good agreement between experimental and calculated dihedral angles for the A-B, C-D and D-A glycosidic linkages. Some deviations are expected from the fibre diffraction data as the molecules are relaxed. These results are described individually in the following sections. Particular attention has been given to those linkages which showed only moderate agreement with the experimental data.

The relaxed conformational energy map for the A-B glycosidic linkage has been included as Figure 2. Two minimum energy conformations were located; these have been

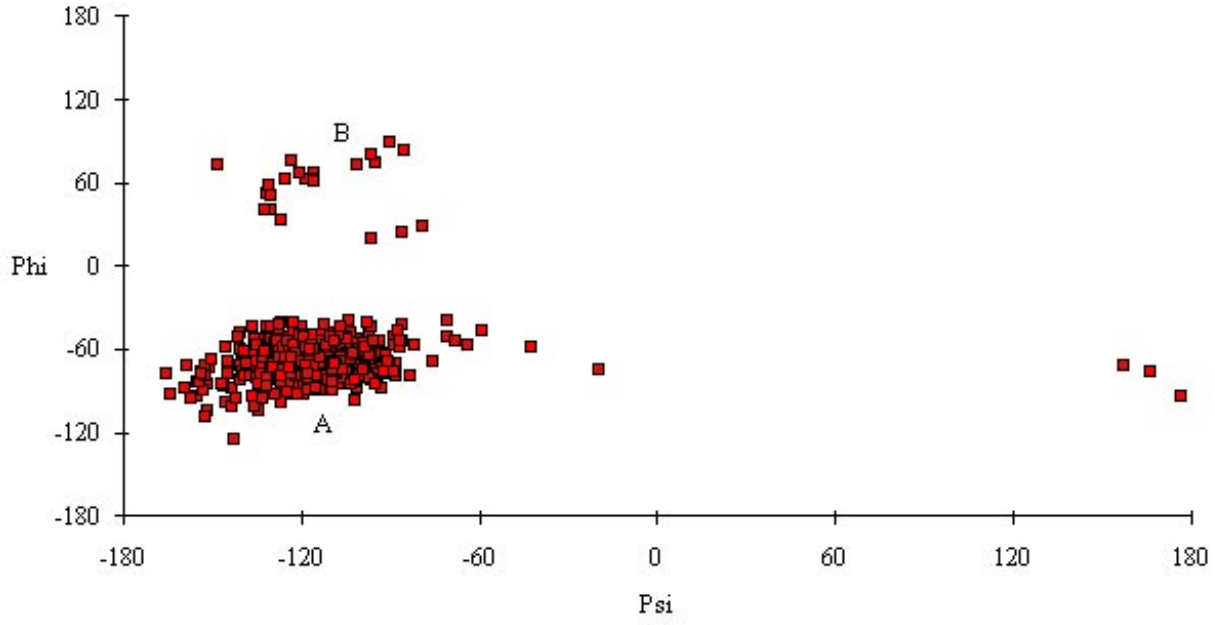

Figure 6. *M.D. simulation of A-B glycosidic linkage, starting from energy well B.*

labelled as energy wells "A" and "B" in Figure 2. The "A" well is located at ϕ = -90°, ψ = -120, which compares favourably with the conformation obtained from the fibre diffraction data of ϕ = -101°, ψ = -136.

The relaxed conformational energy map for the B-C glycosidic linkage revealed two minima. These can be seen in Figure 3. This linkage showed moderate agreement with the fibre diffraction data, almost certainly due to the lack of stabilising interactions from neighbouring residues. This will be discussed in more detail in the section on the MD simulations.

The conformational energy search for the C-D linkage revealed a wide ranging minimum energy well, which is labelled as "A" in Figure 4, and a local minima, "B". The conformation corresponding to "B" is just 1 kcal mol^{-1} above the global minimum at "A". However, neither of these conformations corresponded particularly well to the fibre diffraction data. This is not entirely unexpected, due to the conformational freedom of the rhamnose residue.

The conformational energy map for the D-A linkage showed close agreement with the fibre diffraction data. The conformational energy map for this particular linkage has been included as Figure 5. Two minimum energy conformations have been labelled as "A" and "B".

Disaccharide Simulations with Dielectric Constant

The conformation corresponding to energy well "A" for the A-B glycosidic linkage, see Figure 2, was then used as the starting point for a MD simulation of the A-B disaccharide, as described in the methodology section. During this MD simulation the A-B glycosidic linkage remained in this conformation.

The "B" well in Figure 2 represents a conformation in which the HO3B - O5A hydrogen bond is not topologically possible. This hydrogen bond is an important factor in the formation and stabilisation of the gellan helix; its presence and importance were confirmed by the fibre diffraction data of Chandrasekaran et al. [8]. The MD simulation starting from the conformation associated with the "B" energy well underwent an early transition to the "A" well, where it remained for the remainder of the simulation. These results indicate the importance of this particular hydrogen bond, the formation of which appears to be a major driving force in the helix formation. The MD simulation starting at conformation "B" can be seen in Figure 6, and the HO3B - O5A hydrogen bond can be viewed in Figure 7. The lack of this stabilising influence almost certainly also affected the conformational energy map for the B-C glycosidic linkage.

The global, or over-all, energy minimum for the B-C glycosidic linkage, labelled as "A" in Figure 3 was used as the starting conformation for the MD simulation. The linkage remained in this conformation throughout the MD simulation. When the MD simulation was started at conformation "B", a 10 kcal mol^{-1} energy barrier was crossed early in the simulation, and the linkage remained in the "A" conformation for the remainder of the simulation.

When the crystal structure was used as the starting conformation for a MD simulation for the C-D glycosidic, there was a strong preference for the "B" energy well (see Figure 4). When the "B" energy well conformation was used as the starting conformation, there was a strong preference for the "A" energy well, with only a few transitions to the "B" energy well. This linkage showed only moderate agreement with the fibre diffraction data for the MD simulations; again,

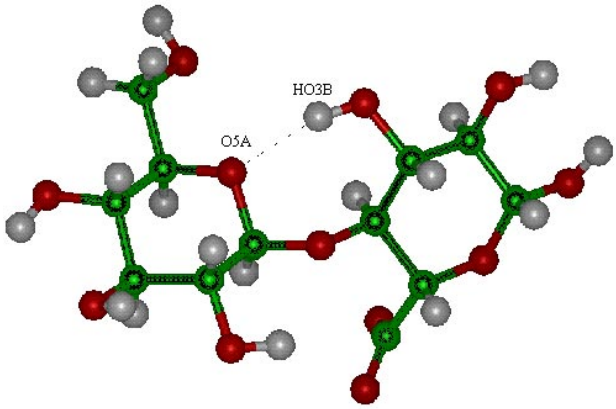

Figure 7. *Representation of HO3B • • • O5A hydrogen bond.*

this is likely to be due to the conformational mobility of the rhamnose residue. The closest low energy conformation to the fibre diffraction data was at ϕ = -150º, ψ = 120º. This was located within 3 kcal mol^{-1} of the minimum energy conformation at "A". However, there were no transitions to this conformation during any of the MD simulations performed.

The fibre diffraction data for the D-A glycosidic linkage is ϕ = -124º, ψ = 88º, which corresponds to the "A" minimum energy well at ϕ = -150º, ψ = 120º (see Figure 5). Two MD simulations were performed for this linkage. The first used the fibre diffraction data as the starting conformation, due its proximity to the "A" energy well. The linkage remained in this conformation throughout the simulation, with no transitions to any other regions.

The second MD simulation used the "B" energy well conformation as the starting conformation. During this simulation the linkage underwent an early transition, during equilibration, to the "A" energy well, where it remained throughout the simulation. The resulting trajectory for this simulation can be viewed in Figure 8. Thus, the D-A glycosidic linkage adopted a stronger preference for the conformation corresponding to the fibre diffraction data than the other three linkages. This is probably due to the reduced flexibility of (1 → 3) compared to (1 → 4) linkages. These results emphasise the importance of the occurrence of the (1 → 3) linkage in the gellan repeat unit for the over-all stability of the helical conformation.

Disaccharide Simulation in Explicit Water

The B-C glycosidic was also minimised in a 15Å^3 box of explicit water molecules, as described in the methods section. This revealed no differences in the location of the minimum energy conformations, although there were differences in the orientations of some of the hydroxyl groups. These results confirm the validity of using implicit solvent in these calculations on disaccharide fragments.

Double Helix Simulations with Ions.

Gellan gel formation at low polysaccharide concentration is dependent on the presence of counter ions. It is believed that they are responsible for the aggregation of the micro-crystalline regions [9]. A qualitative approach has been adopted here in which the ionic interactions are probed in detail. Experimental data to study these interactions are unavailable at

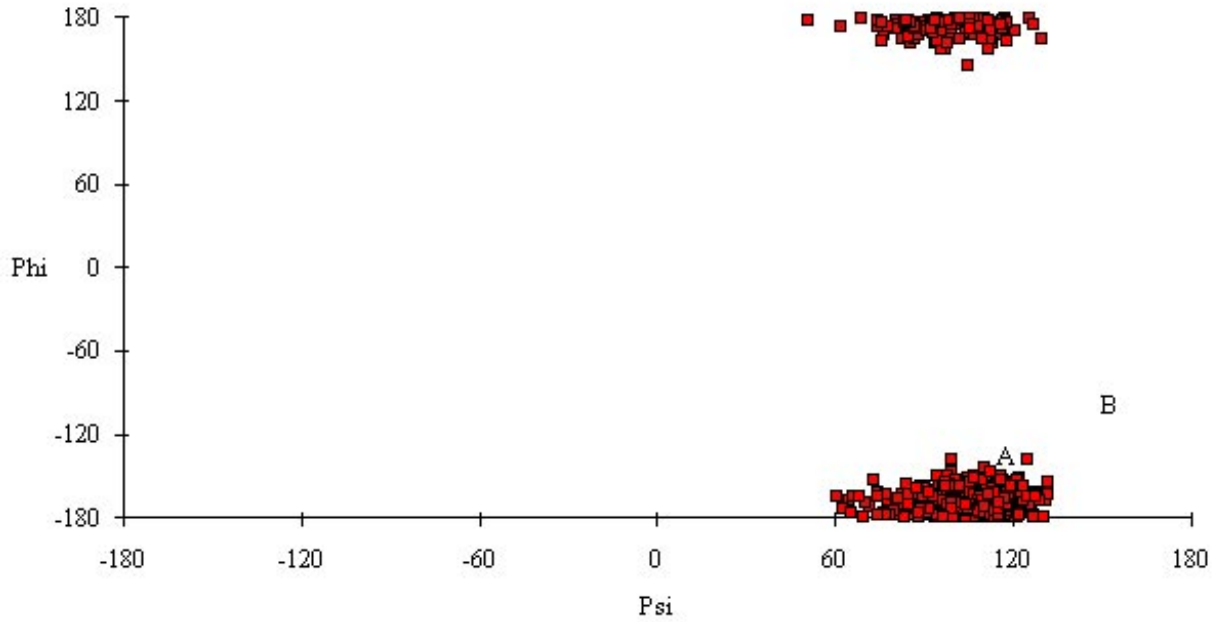

Figure 8. *M.D. simulation of D-A glycosidic linkage, starting from energy well B.*

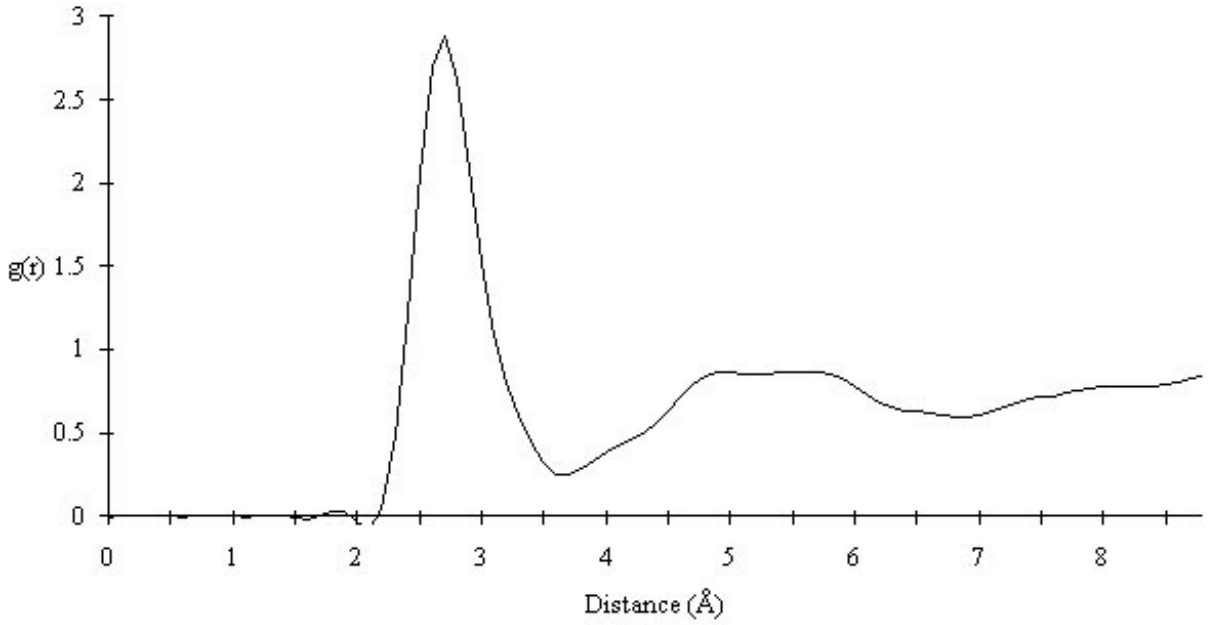

Figure 9. *Pair distribution function for the water molecules around the calcium ion.*

present. The ionic interactions near the carboxyl group are of particular interest, as this is the proposed co-ordination site for the cations. From the MD simulations it should be possible to determine the most favourable positions for the ions to adopt in this region.

Micro-crystalline regions form within aqueous samples of gellan gum. These crystalline regions are thought to be composed of aggregated double helices, based on fibre diffraction data [21]. It is currently believed that the counter ions, which promote gel formation at low polysaccharide concentration, are responsible for the aggregation of these regions [24].

The de-acylated gellan molecule has been reported [21] to form a parallel half-staggered double helix in which each polysaccharide chain is a left-handed 3-fold helix of pitch 56.4 Å. The counter ions known to promote gelation include mono-valent ions such as Li^+, Na^+, K^+ and Cs^+, as well as divalent ions such as Ca^{2+}, Mg^{2+}, Sr^{2+}, Ba^{2+}, Zn^{2+}, Cu^{2+} and Pb^{2+}. Higher concentrations of the monovalent ions are required to produce gels of the strengths produced when divalent counter ions are used. The gel strength for the monovalent ions [7] increases in the order of:

$$Li^+ < Na^+ < K^+ < Cs^+.$$

For divalent ions the corresponding series is:

$$Mg^{2+}, Ca^{2+}, Sr^{2+}, Ba^{2+} < Zn^{2+} < Cu^{2+} < Pb^{2+}.$$

H^+ ions are known to induce gels of higher strengths than even the divalent cations, but the mechanism involved is still unclear. In contrast, large, bulky ions such as tetramethylammonium ions inhibit gel formation; hence they are often included in studies of the dilute solution behaviour of gellan solutions.

The counter ions are believed to be co-ordinated in some way with the carboxyl oxygens of the glucuronic acid residues (labelled as B in Figure 1). In the case of divalent ions, it is believed that the cations bridge directly between two carboxyl oxygens on two double helices [25]. However, the monovalent ions are believed to co-ordinate via water oxygen bridges to the carboxyl oxygens [24].

During the detailed examination of the proposed co-ordination site Ca^{2+} ions were placed near the proposed co-ordination site, which has not been proved experimentally, and a MD simulation was performed, as described earlier. The results from this clearly showed that the ion bridged between the carboxyl oxygens on the two double helices. The average distances during this time were 2.6Å and 2.7Å between the Ca^{2+} ion and the nearest carboxyl oxygen from each double helix. The average distance between these two carboxyl oxygens was 3.1Å. Three water molecules were specifically co-ordinated around the Ca^{2+} ion. The distances between these and the Ca^{2+} were 2.74, 4.64 and 4.92Å respectively.

The van der Waals' and Coulombic interaction energies between the Ca^{2+} ion and the carboxyl oxygens were measured for each binding position of the ion during the MD simulation. This revealed a co-ordination distance of 2.3Å corresponding to the minimum interaction energies observed.

A pair distribution function for the water molecules around the Ca^{2+} ion shows a co-ordination shell of water at about 2.6Å around the ion. This can be seen in Figure 9.

This distance corresponds well to the co-ordination distances reported above between the Ca^{2+} ion and the carboxyl oxygen, and suggests that the water oxygens are replaced by carboxyl oxygens when the ion is co-ordinated with the double helices.

A pair distribution function of the water oxygens around one of the carboxyl oxygens involved in the calcium co-ordination site revealed signs of structuring of the water in this region. Sharp peaks occurred at about 2.8Å, 3.3Å and 3.5Å, and a small peak at 4.4Å, with the continuum beginning at around 5Å. Again, this confirms the important role of the water molecules in these systems. It is also likely that the increase in entropy of the water molecules as they are replaced by the Ca^{2+} ion drives the complex formation, thus leading to gelation. Calculations with monovalent ions are currently in progress, and it will be interesting to compare the structuring of the water in the vicinity of the monovalent bridging ions with that observed here.

Conclusions

In general, the models and force field used here have been shown to reproduce conformations which have been found experimentally. The deviations between experimental crystalline and calculated solvated conformations can be explained in terms of solvation effects and the loss of crystal packing forces.

Several important structural features have been identified. The first of these is the HO3BO5A hydrogen bond, which appears to be one of the main driving forces behind the helix formation. It is interesting to note that this particular feature remains even in the presence of solvent effects.

The second major contribution is the presence of the (13) linkage in the gellan repeat unit. This appears to maintain its stability not only in the crystalline form, but also when solvent is present. Thus it appears to enhance gellan's ability to form, in solution, the helical conformation which is believed to be adopted in the gel state.

We have demonstrated that gellan gel formation is aided by the cation mediated aggregation of double helices. Our results show that divalent cations such as Ca^{2+} can assist in the aggregation of the double helices by directly bridging between carboxyl oxygens. A consequence of this is the formation of ordered micro-crystalline regions, which are necessary for the formation of rigid gels. In addition, some structuring of the water surrounding the binding site was observed.

References

1. Jansson, P.E.; Lindberg B.; Sandford, P.A. *Carbohydrate Research* **1983**, *124,* 135.
2. Graham, H.D. *Journal of Food Science* **1993**, *58* 539.
3. Papageorgiou, M.; Kasapis S.; Richardson, R.K. *Carbohydrate Polymers* **1994**, *25,* 101.
4. Duran, E.; Costell, E.; Izquierdo L.; Duran, L. *Food Hydrocolloids* **1994**, *8,* 373.
5. Crescenzi, V.; Dentini, M.; Coviello T.; Rizzo, R. *Carbohydrate Research* **1986**, *149*, 425.
6. Crescenzi, V.; Dentini, M.; Coviello, T.; Paoletti, S.; Cesàro A.; Delben, F. *Gazetta Chimica Italiana* **1987**, *117,* 611.
7. Grasdalen H.; Smidsrød, O. *Carbohydrate Polymers* **1987**, *7*, 371.
8. Crescenzi, V.; Dentini M.; Dea, I.C.M. *Carbohydrate Research* **1987**, *160*, 283.
9. Gunning A.P.; Morris, V.J. *Int. J. Biol. Macromolecules* **1990**, *12,* 338.
10. Okamoto, T.; Kubota, K.; Kuwahara, N. *Food Hydrocolloids* **1993**, *7*, 363.
11. Tang, J.; Lelievre, J.; Tung, M.A.; Y. Zeng, Y. *Journal of Food Science* **1994**, *59*, 216.
12. Ogawa, E. *Polymer Journal* **1995**, *27*, 567.
13. Moritaka, H.; Nishinari, K.; Taki, M.; Fukuba, H. *Journal of Agriculture and Food Chemistry* **1995**, *43,* 1685.
14. Weiner, S.J.; Kollman, P.A.; Case, D.A.; Chandra, S.U.; Ghio, C.; Alagona, G.; Profeta, S.P.; Weiner, P. *Journal of the American Chemical Society* **1984**, *106,* 765.
15. Homans, S.W. *Biochemistry* **1990**, *29*, 9110.
16. Verlet, L. *Physical Review* **1967**, *159,* 98.
17. Berendsen, H.J.C.; Postma, J.P.M.; van Gunsteren, W.F.; DiNola, A.; Haak, J.R. *Journal of Chemical Physics* **1984**, *81,* 3684.
18. Stern, P.S.; Chorev, M.; Goodman M.; Hagler, A.T. *Biopolymers* **1983**, *22,* 1885.
19. Jorgensen, W.L.; Chandrasekhar, J; Madura, J.D. *Journal of Physical Chemistry* **1983**, *79,* 926.
20. Engelsen, S.B.; Hervé du Penhoat, C.; Pérez, S. *Journal of Physical Chemistry* **1995**, *99,* 13334.
21. Chandrasekaran, R.; Puigjaner, L.C.; Joyce, K.L.; Arnott, S. *Carbohydrate Research* **1988**, *181,* 23.
22. Chandrasekaran, R.; Radha, A. *Trends in Food Science and Technology* **1995**, *6,* 143.
23. Chandrasekaran, R.; Millane, R.P.; Arnott S.; Atkins, E.D.T. *Carbohydrate Research* **1988**, *175,* 1.
24. Chandrasekaran, R.; Radha, A.; Thailambal, V.G. *Carbohydrate Research* **1992**, *224,* 1.
25. Chandrasekaran, R. *Advances in Experimental Medical Biology* **1991**, *302,* 773.